ACS APPLIED MATERIALS & INTERFACES

Research Article

www.acsami.org

Nickel–Aluminum Layered Double Hydroxide Coating on the Surface of Conductive Substrates by Liquid Phase Deposition

Hideshi Maki,* Masashi Takigawa, and Minoru Mizuhata

Department of Chemical Science and Engineering, Graduate School of Engineering, Kobe University, 1-1 Rokkodai-cho, Nada-ku, Kobe 657-8501, Japan

Supporting Information

ABSTRACT: The direct synthesis of the adhered Ni–Al LDH thin film onto the surface of electrically conductive substrates by the liquid phase deposition (LPD) reaction is carried out for the development of the positive electrode. The complexation and solution equilibria of the dissolved species in the LPD reaction have been clarified by a theoretical approach, and the LPD reaction conditions for the Ni–Al LDH depositions are shown to be optimized by controlling the fluoride ion concentration and the pH of the LPD reaction solutions. The yields of metal oxides and hydroxides by the LPD method are very sensitive to the supersaturation state of the hydroxide in the reaction solution. The surfaces of conductive substrates are completely covered by the minute mesh-like Ni–Al LDH thin film; furthermore, there is no gap between the surfaces of conductive substrates and the deposited Ni–Al LDH thin film. The active material layer thickness was able to be controlled within the range from 100 nm to 1 μm by the LPD reaction time. The high-crystallinity and the arbitrary-thickness thin films on the conductive substrate surface will be beneficial for the interface control of charge transfer reaction fields and the internal resistance reduction of various secondary batteries.

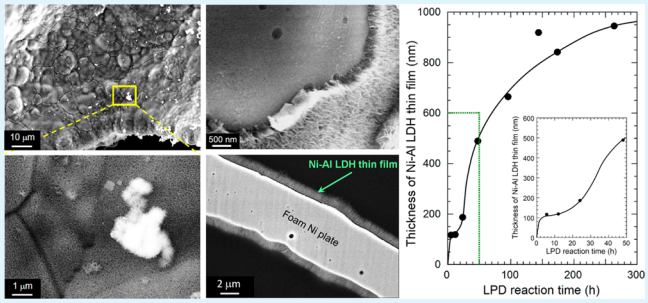

KEYWORDS: *LDH, layered double hydroxide, liquid phase deposition, LPD, Ni–Al LDH, charge transfer resistance, Ni-MH battery, current collector*

1. INTRODUCTION

The Ni–metal hydride (NiMH) battery, in which the electrolytic solution is an aqueous solution, is safer than the Li-ion battery, in which the electrolytic solution is an inflammable organic solvent. The positive active material for the Ni-MH secondary battery widely used at present is β-$Ni(OH)_2$. If α-$Ni(OH)_2$ is applied in the positive electrode reaction of a Ni-MH battery, the volumetric change of the active material during the charge/discharge processes will be small, and the positive electrode capacity can be drastically improved.[1,2] However, α-$Ni(OH)_2$ is very chemically unstable in strongly alkaline solutions. Consequently, the Ni–Al layered double hydroxide (LDH), in which some of the Ni^{2+} ions which form the main framework in the LDH are substituted by Al^{3+} ions, has been proposed.[3−13]

The general structural formula of an LDH is $[M_{1-x}^{2+}M_x^{3+}(OH)_2]^{x+}[A_{x/n}^{n-}\cdot yH_2O]^{x-}$ (M^{2+}; Ni^{2+}, Mg^{2+}, Zn^{2+}, Co^{2+}, etc., M^{3+}; Al^{3+}, Cr^{3+}, Fe^{3+}, Co^{3+}, and so forth, A^{n-}; OH^-, Cl^-, NO_3^-, CO_3^{2-}, SO_4^{2-}, and so forth),[14−22] and the LDHs have a crystal structure in which some of the bivalent metal cations are substituted for trivalent metal cations. Synthetic methods involving homogeneous reaction systems, such as the hydrolysis reaction (e.g., a sol–gel method), the dehydrative condensation reaction, and the coprecipitation method, have been reported for the LDHs.[21,23−29] However, the crystallinities of the LDHs which were synthesized by such conventional methods are low, and alkali metals as impurities are incorporated into the crystal structure of the LDHs. The liquid phase deposition (LPD) method is a metal oxide and hydroxide synthesis procedure using the hydrolysis equilibria reactions of metal-fluoro complexes, and the LDHs with high crystallinities and purity can be synthesized, as no alkali cations are present in the LPD reaction solutions. Accordingly, the LPD method has been proposed as a novel synthetic procedure for LDHs.[7−12,14] The LPD method enables a simple synthesis of nickel hydroxide with a stable α-phase in strongly alkaline solutions by the introduction of trivalent cations to the main frames in the LDH. Moreover, the syntheses of various active materials to the surfaces on substrates of various materials which have complicated surface shapes (e.g., fine particles and inner wall of small pores) are possible using the LPD method. In our previous study, the Ni–Al LDH thin film was deposited onto the hydrophilic α-alumina powder surface by the LPD method, and the pH and the fluoride ion concentration dependences in the LPD reaction solution on the deposition amount of the Ni–Al LDH thin film were investigated.[14] In addition, we recently attempted the synthesis of Ni–Al LDH onto the surfaces of various conductive materials using the LPD

Received: May 10, 2015
Accepted: July 18, 2015
Published: July 18, 2015

DOI: 10.1021/acsami.5b04038
ACS Appl. Mater. Interfaces 2015, 7, 17188−17198

method, and as a result, the Ni−Al LDH coating onto the surface of carbon black powder, which is the conductive auxiliary for secondary battery electrodes, was achieved. The positive electrode for a Ni-MH battery was constructed by using this carbon black core Ni−Al LDH as an active material, and its electrochemical characteristic was evaluated.[8−12] This positive electrode showed excellent charge/discharge characteristics, and a discharge capacity of above 380 mAh g^{-1} was retained after 869 charge/discharge cycles.[9] However, the adhesion between the active materials and between current collectors and active materials in this positive electrode was poor; thus, this was the cause for the charge transfer resistance. The reduction of the battery internal resistance is important for the development of low cost and long life secondary batteries.[30−34] A reduction of the internal resistance enables a reduction of the heat deterioration of the electrode materials and an acceleration of the charge/discharge speed of the batteries. Therefore, to develop a positive electrode that possesses high capacity and low charge transfer resistance, the direct synthesis of the Ni−Al LDH onto the surface of electrically conductive substrates by the LPD reaction was carried out in this work.

The LPD reaction field is only the solid−liquid interface, although the LPD reaction applies a competitive complexation equilibria in an aqueous solution. This is to say the reaction products deposit by the interfacial reaction which continuously forms the thin film only on the surface of a solid phase.[35−39] Hence, it can be considered that the solution condition of the LPD reaction for the high yield synthesis of Ni−Al LDH is not affected by the material or shape of the substrates. However, the wettability of the substrate surface has a large influence on the amount of Ni−Al LDH deposited on the surface. A foam nickel plate, which can act as a current collector in Ni-MH secondary batteries, is used as a substrate in this research, as it possesses high electric conductivity and low hydrophilic surface; hence, the surface hydrophilization treatment to improve the wettability of the LPD reaction solution is indispensable. On the other hand, the active material layers which are adhered to the substrates can be constructed using the LPD method. Accordingly, the charge transfer resistance between a current collector and an active material can be expected to be drastically decreased when a current collector is used as a substrate. Hence, direct deposition of LDHs on conductive substrates as current collectors[40,41] can drastically reduce the interface charge transfer resistance between the current collectors and active materials. Furthermore, in this work, the hydrolysis reaction and the fluoride ion consumption reaction in the LPD reaction, which had been empirically carried out, were considered from the viewpoint of the reaction equilibria of the metal fluoride complexations. Hence, the LPD reaction condition for the Ni−Al LDH deposition onto the surface of a foam nickel plate as a current collector for the Ni-MH battery was optimized by controlling the fluoride ion concentration and the pH. Therefore, research regarding the optimal solution conditions for the LPD reaction can be applied to the construction of electrode systems possessing low internal resistances which control high-order nanostructures.[30−34]

2. EXPERIMENTAL SECTION

2.1. Chemicals. All chemicals used in this work were of analytical grade. Hydrofluoric acid, an aqueous solution of HF, was purchased from Stella Chemifa Corporation and all other reagents were purchased from Nacalai Tesque Inc. The properties of carbon black powder (Mitsubishi Chemical Corp., 3050B) is following: particle diameter is ca. 4 μm, and BET surface area is 65.9 $m^2\ g^{-1}$. The carbon black powder was preheated above 1000 °C. The properties of foam nickel plate (Sumitomo Electric Industries, Ltd., Celmet #8) is following: mean bore diameter is 0.45 mm, specific surface area is 291 $cm^2\ g^{-1}$, porosity is 98%, and all pores are through holes. The foam nickel plate has been manufactured as follows: after electric conductive treatment to urethane foam, metal nickel was electrodeposited to the urethane foam, and finally, the urethane foam substrate was incinerated by a heat-treatment. The carbon black powder and foam nickel plate were treated with a hydrophobizing process by ozone irradiation for 45 min (Ebara Jitsugyo Co. Ltd., EKBIO-1100) and argon plasma irradiation (Gala Gabler Labor Instrumente Handels GmbH, Plasma Prep2) for 30 min, respectively.

2.2. Preparation of Ni−Al LDH on Various Conductive Subsrates by the LPD Reaction. Ni parent solution for the LPD reaction was prepared in accordance with our previous report[14] (i.e., section 2.3.1 in ref 14) as shown in Scheme S1. The total concentration of Ni^{2+} ion in this solution was determined by an inductively coupled plasma optical emission spectrometry (ICP-OES; HORIBA Ltd., ULTIMA 2000). Appropriate amount of the fluoride complex solution was diluted by pure water, the total concentration of fluoride ion was adjusted by 0.5 mol L^{-1} HF, the pH of the solution was also adjusted by 0.2 mol L^{-1} ammonia−water, finally, 1.0 mol L^{-1} $Al(NO_3)_3$ aqueous solution was added up to the prescribed concentration of Al^{3+} ion which is a fluorine scavenger, and the Ni parent solution for the LPD reaction was obtained. The concentration condition of the Ni parent solution was as follows: the total concentration of Ni^{2+} ion, Al^{3+} ion, and F^- ion were 12 mmol L^{-1}, 1.2 mmol L^{-1}, and 70−500 mmol L^{-1}, respectively, and the pH range was 7.5−8.3. Twenty mg of hydrophilization treated carbon black powder or 6 cm^2 of foam nickel plate as conductive substrates by ozone oxidation with Ozone/UV surface treatment system (Ebara Jitsugyo Co., Ltd., EKBIO-1100) were added or suspended vertically into 100 mL of this parent solution, and reacted at 50 °C for the predetermined time. The substrates were retrieved from the LPD reaction solution, washed with distilled water, and dried at room temperature, and finally, the Ni−Al LDH on carbon black powder and the Ni−Al LDH on foam nickel plate were prepared.

2.3. Characterization of Deposited Ni−Al LDH Thin Films. The crystalline structures of Ni−Al LDH thin films on conductive materials were investigated using an X-ray diffractometer (XRD; Rigaku Corp., RINT-TTR/S2) in accordance with our previous report.[14] The amounts of Ni deposited on carbon black powder were measured by the ICP-OES. The samples of the depositions were dissolved into dilute nitric acid. Standard nickel solution with a concentration of 1000 ppm was used as reference samples. The surface morphologies and the cross-section images of the Ni−Al LDHs on carbon black powder and on foam nickel plate were observed by a field emission scanning electron microscope (FE-SEM; JEOL Ltd., JEM-6335F) in accordance with our previous report.[14] An EDX elemental mapping analyzer (JEOL Ltd., EX-23000BU) was used to elucidate the distribution of Ni and Al. The sample for the cross-sectional SEM observation was fabricated as follows: The Ni−Al LDH on carbon black powder or a small sample of Ni−Al LDH on foam nickel plate was kneaded with thermosetting epoxy resin, and was filled to a hole of 3 mm in diameter and 1.5 mm in depth which was made on an acrylic plate of 4 mm in thickness, and then the acrylic plate was heated for 12 h at 70 °C to be solidified. The cross sections of the solidified observation samples were exposed by the cutting off an acrylic board using a low speed cutter (Buehler, IsoMet), and then it was exactly smoothed by the irradiating and etching of a focusing argon ion beam for 24 h at the vicinity of a sample cross section region using a cross section polisher (JEOL Ltd., SM-09010).

3. RESULTS AND DISCUSSION

3.1. Complexation and Dissolution Equilibria in the LPD Reaction. The LPD method involves a metal oxide and

DOI: 10.1021/acsami.5b04038
ACS Appl. Mater. Interfaces 2015, 7, 17188−17198

hydroxide thin films synthetic procedure using the hydrolysis equilibria reactions of metal-fluoro complexes. The LPD reaction spontaneously proceeds at ambient conditions in a balance of two equilibrium reactions, which are principally described as follows;[35−39]

$$MF_x^{(x-2n)-} + H_2O \rightarrow MO_n + xF^- + 2nH^+$$
(M; e. g. , Ti, Fe, Cu, Zr, Sn, W, Mo, V, Zr, Nb, Ni) (1)

$$H_3BO_3 + 4HF \rightarrow BF_4^- + H_3O^+ + 2H_2O \quad (2)$$

$$Al^{3+} + 6HF \rightarrow H_3AlF_6 + 3/2H_2 \quad (3)$$

The addition of an F^- scavenger (e.g., H_3BO_3 or Al^{3+}) leads to the consumption of F^- ions eq 2 or 3) and the hydrolysis reaction (eq 1) is shifted in the direction of the metal oxide deposition. Thus, the shape and the composition of the synthesized metal oxides depend on the pH of LPD reaction solutions and the concentrations of metal ion and fluorine scavenger. A drastic reduction in the manufacturing cost and energy is possible, owing to its simple experimental procedure and mild reaction conditions compared with the conventional method (e.g., the vapor-phase method). In addition, the LPD method, which involves solution reactions, is a film production procedure that has attracted great interest in recent years because of its ability to deposit metal oxide thin films on substrate surfaces which have large areas and complicated shapes.[14,39,42−44] The stability constants of various metal-fluoro complexes, K_n, involved in LPD reactions are shown in Figure S1 (Supporting Information).[45,46] The boron and the Al^{3+} ion function as a fluoride ion consumption remedy in the LPD reaction solution because the stability constants of their fluoro complexes are very high. High valence metal ions, such as Ti^{4+}, Zr^{4+}, Fe^{3+}, and so forth, have oxide thin films, such as the TiO_2, ZrO_2, FeOOH, and so forth, which are easily synthesized by liquid phase deposition, also forming stable fluoride complexes.[35,36,47] Information regarding the solution equilibria of the dissolved species in the LPD reaction will be clarified in this research. Additionally, the fluoride complexes of divalent 3d metal ions, which are "soft" cations according to the HSAB concept, are not formed in the solution in which the concentration of fluoride ions is low.[48−51] Therefore, the coordination number of the fluoride ion in the dissolution state is not high. Thus, increasing the fluoride ion concentration is necessary to synthesize the oxide thin films of divalent 3d metal ions using the LPD method. In the reaction observed at a high concentration of fluoride ions, the side reaction, which is the precipitate formation of the metal hydroxide by the liquid phase reaction at all reaction fields except the surface of the substrates, may be rapidly generated. Therefore, the stabilization of the supersaturation state of the metal hydroxide in the LPD reaction solution and the control of the LPD reaction rate are very important for the synthesis of metal oxides or hydroxides by the LPD method.

In this work, we have treated the hydrolysis reaction and the fluorine scavenging reaction in the LPD reaction from the viewpoint of the nickel fluoride complexation and the solubility product of β-$Ni(OH)_2$. The solubility product of β-$Ni(OH)_2$, k_{sp}, is defined as follows;

$$k_{sp} = [Ni^{2+}][OH^-]^2 \quad (4)$$

The pH dependence of the solubility of β-$Ni(OH)_2$ in aqueous solution is expressed by eq 5.

$$[Ni^{2+}] = 10^{2(14-pH)}k_{sp} \quad (5)$$

To deposit nickel hydroxide using the LPD reaction, a higher concentration of the total concentration of the nickel ion than that shown by eq 5 is required by the dissolution of nickel fluoride. The "soft" cations, according to definition of the HSAB concept, such as the Ni^{2+} ion, hardly form stable complexes with the F^- ion, which is considered to be a "hard" anion.[48−51] The successive stability constants after the k_2 values for nickel fluoride complexes are negligibly small. Thus, the overall stability constant of the nickel fluoride complex, K, can be expressed by the following equation;

$$K = [NiF^+]/([Ni^{2+}]\cdot[F^-]) \quad (6)$$

Namely, all nickel dissolves under the concentration conditions provided in the following equation;

$$[NiF^+] > C_{Ni} - [Ni^{2+}] = C_F - [F^-] \quad (7)$$

where C_{Ni} and C_F are the total concentrations of nickel and fluorine, respectively. From eqs 6 and 7:

$$[F^-] > (C_{Ni} - [Ni^{2+}])/(K\cdot[Ni^{2+}]) \quad (8)$$

Finally,

$$C_F > (C_{Ni} - [Ni^{2+}])/(K\cdot[Ni^{2+}] + (C_{Ni} - [Ni^{2+}])) = (C_{Ni} - 10^{2(14-pH)}\cdot k_{sp})(1 + 1/10^{2(14-pH)}\cdot k_{sp}\cdot K) \quad (9)$$

Therefore, the solution equilibria of the nickel fluoride complex can be uniquely expressed by the C_{Ni}, C_F, and the pH of the LPD reaction solution. Figure 1 shows the solubility diagram of nickel hydroxide at various pH values and the concentration of fluorine at a constant value of C_{Ni}. There is a clear difference between the theoretical value and the experimental result because of the decrease in the solubility of β-$Ni(OH)_2$, owing to the decrease in the dissociation degree of HF in the low pH range, and the formation of polynuclear complex, owing to the

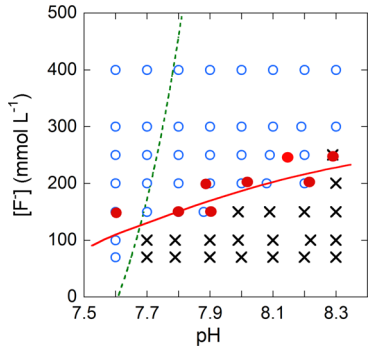

Figure 1. Solubility diagram of nickel hydroxide at various pH values and the concentration of F^- ion. Each point shows the result of the experiment of hydrolysis of nickel fluoride complex. C_{Ni} = 12 mmol L^{-1}, $k_{sp} = 2 \times 10^{-15}$ mol^3 L^{-3}, $k_1 = 10^{0.5}$. The red solid line shows the smooth curve of the result of the practical synthesis conditions for Ni/Al-LDH by the LPD reaction (i.e., the key of closed red circle), and the green dashed line refers to the calculated solution equilibria curve of nickel fluoride complex by eq 9. Key: (blue open) soluble; (×) forming hydroxide precipitation; (red closed) practical synthesis condition for Ni/Al-LDH by the LPD reaction.

DOI: 10.1021/acsami.5b04038
ACS Appl. Mater. Interfaces 2015, 7, 17188−17198

bridging by OH^- ions in the high pH range. However, the experimental results are approximately identical to the experimental deposition behavior of the Ni−Al LDH by the LPD method as described in Sections 3.2 and 3.3. Therefore, the diagram can be applied as a benchmark for the influence of the fluoride concentration and the pH of the LPD reaction solution for the Ni−Al LDH synthesis by the LPD method.

3.2. Influence of the LPD Reaction Solution Condition on the Ni−Al LDH Deposition Behavior to Carbon Black Powder. Figure 2 shows the XRD patterns of the deposited

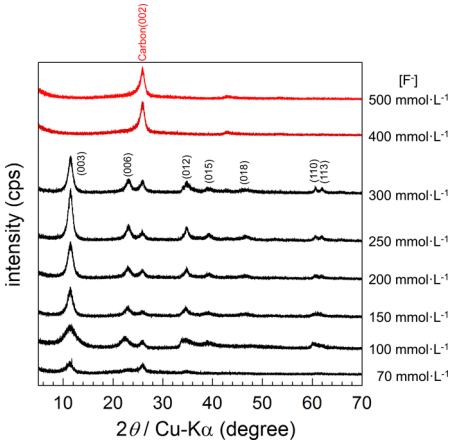

Figure 2. X-ray diffraction patterns of Ni−Al LDH thin films on the surface of carbon black powder deposited by the LPD reaction at 50 °C for 48 h and obtained at various total concentrations of fluorine. The pH of the LPD reaction solution is 8.2, and the concentrations of Ni^{2+} ion and Al^{3+} ion were 12 mmol L^{-1} and 1.2 mmol L^{-1}, respectively.

Ni−Al LDH thin films on the surface of carbon black powder by the LPD method over a reaction time of 48 h at different total concentrations of fluorine. Aluminum of approximately 18 mol % is doped to the Ni−Al LDH at an Al concentration, C_{Al}, of 1.2 mmol L^{-1}. The obtained Ni−Al LDH is the most chemically stable, and the electrochemical properties are the most superior.[8] It should be noted that the deposition behavior and the crystallinity of the Ni−Al LDH are dependent on the fluoride concentration in the LPD reaction solution. The highly crystalline Ni−Al LDH is deposited by the LPD reaction in the concentration range of $[F^-]$ = 150−300 mmol L^{-1}. The width of the (003) XRD reflection is large in the concentration range of $[F^-]$ < 100 mmol L^{-1}; namely, the crystallinity of the deposited Ni−Al LDH is low in this concentration range. Moreover, the Ni−Al LDH is scarcely obtained in the concentration range of $[F^-]$ > 400 mmol L^{-1}, because the formation of the nickel fluoride increases as the F^- scavenger cannot scavenge fluorine sufficiently from the nickel ion at this high concentration range. The composition dependence of the LPD reaction solution on the deposition behavior and the crystallinity of the Ni−Al LDH is in good agreement with the solubility diagram of nickel hydroxide at various pH values and the concentration of fluorine, which is discussed in Section 3.1.

Figure 3 (top) shows the pH dependence of the XRD patterns of the Ni−Al LDH thin films on the surface of carbon black powder obtained by the LPD process at various total concentrations of fluorine. All detected peaks showed the same diffraction characteristics as Ni−Al LDH,[14] and no peaks arising from α-$Ni(OH)_2$ or β-$Ni(OH)_2$ were detected. The peak intensity of Ni−Al LDH samples is affected by the pH of the

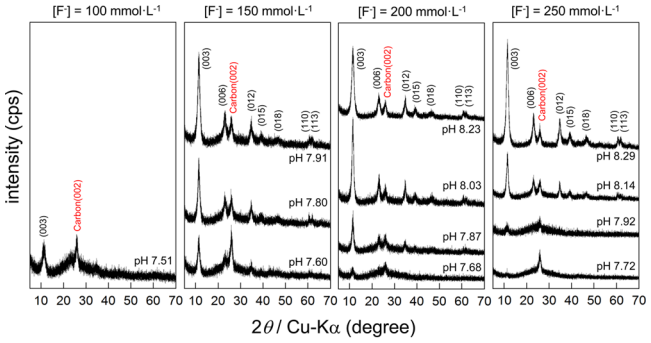

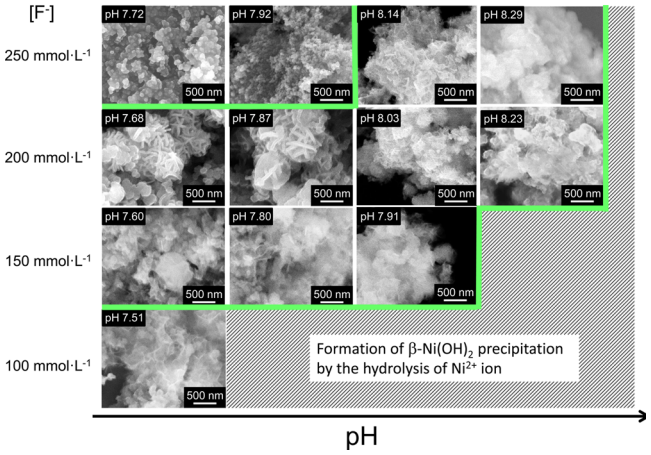

Figure 3. X-ray diffraction patterns (top) and surface morphologies by SEM (bottom) of the Ni−Al LDH thin films on the surface of carbon black powder deposited by the LPD reaction at 50 °C for 48 h and obtained at various pH values and total concentrations of fluorine. The concentrations of Ni^{2+} ion and Al^{3+} ion were 12 mmol L^{-1} and 1.2 mmol L^{-1}, respectively.

LPD reaction solution. In summary, the crystallinity and the deposition amount of Ni−Al LDH depend on the pH of the LPD reaction solution. In the low pH region (i.e., pH < 7.7), the crystallinity of obtained Ni−Al LDH is low, and the yield is poor. This low pH region is unsuitable as a high crystalline Ni−Al LDH synthesis condition, because the nickel fluoride complex, which is a precursor of Ni−Al LDH, is hardly formed, owing to the decrease in the dissociation degree of HF in the low pH range.[36] Additionally, the high pH region (i.e., pH > 8.4) is also unsuitable for Ni−Al LDH synthesis, because of the precipitation of a polynuclear complex, owing to the bridging by OH^- ions observed at a high pH. In the case of an LPD reaction solution of 7.8 < pH < 8.3, the crystallinity of the obtained Ni−Al LDH is relatively high and the yield is improved. The pH dependence of the LPD reaction solution on the deposition behavior and the crystallinity of the Ni−Al LDH is in good agreement with the discussion in Section 3.1 as well as the concentrations of the dissolved species in the LPD solution. SEM micrographs of Ni−Al LDH on carbon black powder, which was prepared under the same experimental conditions, are shown in Figure 3 (bottom). In the SEM images, many irregular plate-like particles of Ni−Al LDHs of more than 150 nm in diameter and 50 nm in thickness form densely on the surface of carbon black powder in the pH range of 7.6 < pH < 8.3. The surface morphology and the particle size of these Ni−Al LDHs are almost the same as those of Ni−Al LDH prepared on the surface of α-alumina powder in our

DOI: 10.1021/acsami.5b04038
ACS Appl. Mater. Interfaces 2015, 7, 17188−17198

previous report.[14] It is reasonable to suppose that neither the surface characteristics nor the particle size of the LPD reaction products depend on the material and the shape of the substrates, because the LPD method is a reaction in solution using the minute free energy difference between two complexation equilibria as a driving force for the progress of the reaction, as described in Section 3.1. However, the preparation of the Ni−Al LDH cannot be confirmed for the LPD reaction solutions of pH 7.51 at $[F^-]$ = 100 mmol L^{-1} and pH 7.72 and 7.92 at $[F^-]$ = 250 mmol L^{-1}. The surface morphology and the particle size depend on the pH and the dissolved species concentrations of the LPD reaction solution as well as the crystallinity of the Ni−Al LDH.

Figure 4 shows the dependence of pH and the total fluoride concentrations of the LPD reaction solution on the deposition

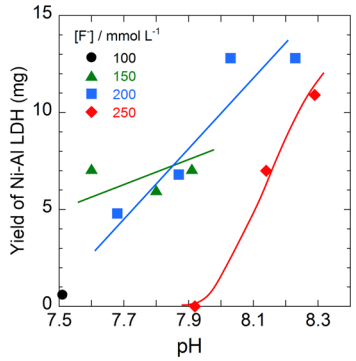

Figure 4. Total concentration of fluorine and the pH of the LPD reaction solution dependence of the deposition amount of Ni−Al LDH thin films on the surface of carbon black powder by the LPD reaction. The other condition of the LPD reaction solution is as in Figure 2. Total concentrations of fluorine in the LPD reaction solution: (●) 100 mmol L^{-1}; (▲) 150 mmol L^{-1}; (■) 200 mmol L^{-1}; (◆) 250 mmol L^{-1}. Solid lines show smooth curves between data points.

amount of Ni−Al LDH thin films on the surface of carbon black powder which was observed by the ICP-OES. It is observed that the yield of the Ni−Al LDH decreases for the LPD reaction solution of the low fluoride concentration (i.e., $[F^-]$ = 100 mmol L^{-1}) and the low pH region (i.e., pH < 7.7). Figure 3 shows the results of XRD and SEM. The yield of the Ni−Al LDH considerably depends on the pH and the total fluoride concentration of the LPD reaction solutions as well as the surface morphology and the particle size. It is remarkable that a weak driving force, such as a moderate change in pH of a reaction solution, gives rise to such a drastic change of the yield, the surface morphology, and the particle size of the reaction product. The deposition amount of the Ni−Al LDH increases remarkably in the range of pH > 8, whereas the precipitation of β-$Ni(OH)_2$ becomes predominant in the range of pH > 8.5. Therefore, the supersaturated state of nickel hydroxide is presented in the range of 8.2 < pH < 8.5, and the Ni−Al LDH deposits at the solid−liquid interface reaction, where a thin film deposits only on the substrate surface. Consequently, it can be concluded from the above discussions that Ni−Al LDH of the highest yield and crystallinity can be synthesized by the LPD reaction at pH 8.2 and $[F^-]$ = 200 mmol L^{-1} ($[F^-]/[Ni^{2+}]$ = 200 mmol L^{-1}/12 mmol L^{-1} = 16.7). These optimal synthesis conditions will be observed immediately before β-$Ni(OH)_2$ precipitates in the LPD reaction solution, that is, a solution condition in which nickel hydroxide is in a supersaturated state.

It can be expected that this optimal synthesis condition depends minimally on the material and the surface shape of solid substrates, because the LPD reaction progresses only by the reaction in solution. According to our previous research, which used α-alumina powder, the highest yield of Ni−Al LDH thin film was achieved by the LPD reaction at pH 7.8 and $[F^-]/[Ni^{2+}]$ = 16.7 (i.e., 200 mmol L^{-1}/12 mmol L^{-1}).[14] The dominant progress of the deposition reaction in a high fluoride concentration and low pH region suggests that the Ni−Al LDH stabilizes at the solid−liquid interface in the case of α-alumina powder substrates, and it can be considered that the hydrophilic property of substrates contributes to the stabilization of the Ni−Al LDH. Hence, it can be concluded that the hydrophilization of substrates contributes not only to the improvement of the wettability on the substrate surface but also the direct acceleration of the thin film deposition. If the stability of the fluoride complex of the metal ion, which is the "soft" cation according to the HSAB concept[48−51] (e.g., Ni, Co, Cu, Fe, and so forth), as the precursor of the LPD reaction is low, the high yield syntheses of the high-crystallinity metal oxides and hydroxides by the LPD method will be possible by the control of the hydrolysis equilibria through the optimal control of the concentration of fluoride ions and the pH of the reaction solution.

The deposition amount of the Ni−Al LDH is also controllable by the LPD reaction time. Figure 5 shows the

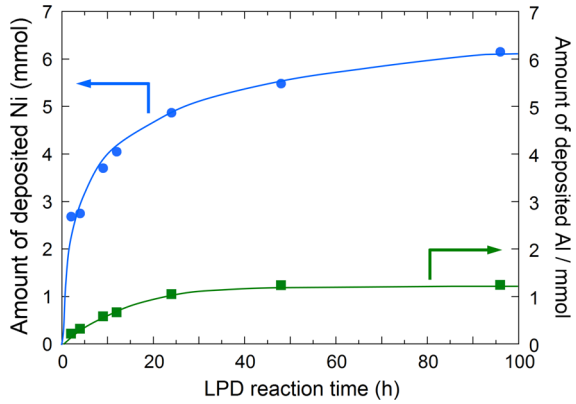

Figure 5. Reaction time dependence of the deposition amounts of Ni and Al on the surface of carbon black powder by the LPD reaction. The pH of the LPD reaction solution is 8.2, the concentrations of Ni^{2+} ion and Al^{3+} ion were 12 mmol L^{-1} and 1.2 mmol L^{-1}, respectively, and the total concentration of fluorine is 200 mmol L^{-1}. Key: (●) deposition amount of Ni; (■) deposition amount of Al. Solid lines show smooth curves between data points.

reaction time dependence of the deposition amount of Ni and Al on the surface of carbon black powder under the optimal LPD reaction conditions. The deposition amounts of both Ni and Al reach a constant with an LPD reaction time of about 100 h. The deposition rates of Ni and Al are not constant, and the deposition of approximately 80% is completed after 24 h. It should be noted that the ratio of the deposition amounts of Ni and Al does not depend on the reaction time and is almost constant; namely, the composition formula of the Ni−Al LDH on carbon black powder was $Ni_{0.77}Al_{0.23}(OH)_2 \cdot X_{0.23}$ (X means the ion exchangeable OH^- anions between the LDH layers), and this result was in good agreement with our previous research.[8,9,12] This suggests that segregation does not occur and the deposited Ni−Al LDH has an almost uniform composition.

DOI: 10.1021/acsami.5b04038
ACS Appl. Mater. Interfaces 2015, 7, 17188−17198

This might be related to the high density of the Ni−Al LDH prepared by the LPD method. Figure 6 shows the cross-sectional SEM image of the Ni−Al LDH on carbon black powder. The Ni−Al LDH, of film thickness about 900 nm, deposits on the carbon black powder with an average primary particle diameter of approximately 4 μm. The carbon black powder surface is completely coated with the deposited Ni−Al LDH, and no void exists between the Ni−Al LDH and the carbon black powder surface. Hence, the deposited Ni−Al LDH and the powder surface will be kept in contact with each other. This is a consequence of the Ni−Al LDH deposited by the interfacial reaction, where the thin film forms only on the surface of the solid phase since the reaction field of the LPD method is a solid−liquid interface.

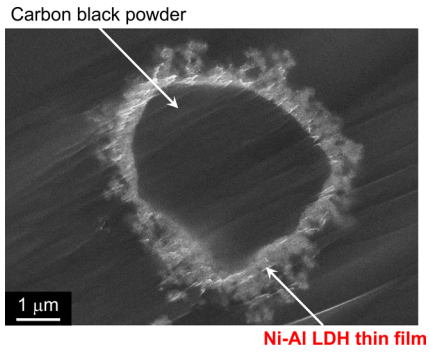

Figure 6. Cross-sectional SEM image of the Ni−Al LDH on carbon black powder. The LPD reaction time is 48 h. The other condition of the LPD reaction solution is as in Figure 4.

3.3. Influence of the LPD Reaction Solution Conditions on the Ni−Al LDH Deposition Behavior to Foam Nickel Plate. Carbon black powder has a rough surface, and a minute irregular structure on the nano-order exists on the surface. Hence, there are innumerable starting points for the very early stage deposition of Ni−Al LDH on the surface. Therefore, the Ni−Al LDH deposition by the LPD reaction on the surface of carbon black powder was completed in a short time, as was also observed for α-alumina powder. However, the starting points for the early stage in the Ni−Al LDH deposition on a foam nickel plate are much fewer than those on carbon black powder and the α-alumina powder, because of the high surface smoothness of the foam nickel plate as shown in Figure S2 (Supporting Information). Consequently, the deposition rate of Ni−Al LDH on the foam nickel plate surface is expected to decrease. In addition, the surface area per unit volume of the foam nickel plate is smaller than those of carbon black powder

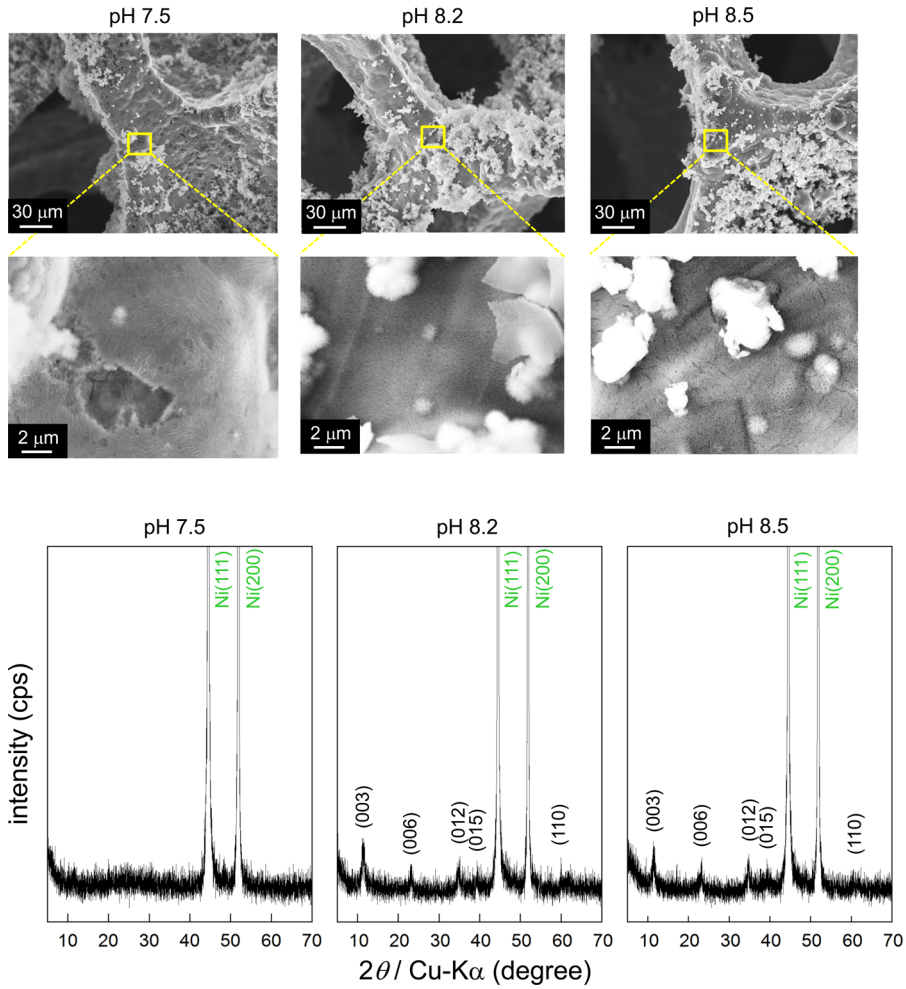

Figure 7. Surface morphologies by SEM (top) and X-ray diffraction patterns (bottom) of Ni−Al LDH thin films on the surface of foam nickel plates deposited by the LPD reaction at 50 °C for 48 h and obtained at various pH values. The concentrations of Ni^{2+} ion and Al^{3+} ion were 12 mmol L^{-1} and 2.0 mmol L^{-1}, respectively, and the total concentration of fluorine is 200 mmol L^{-1}.

DOI: 10.1021/acsami.5b04038
ACS Appl. Mater. Interfaces 2015, 7, 17188−17198

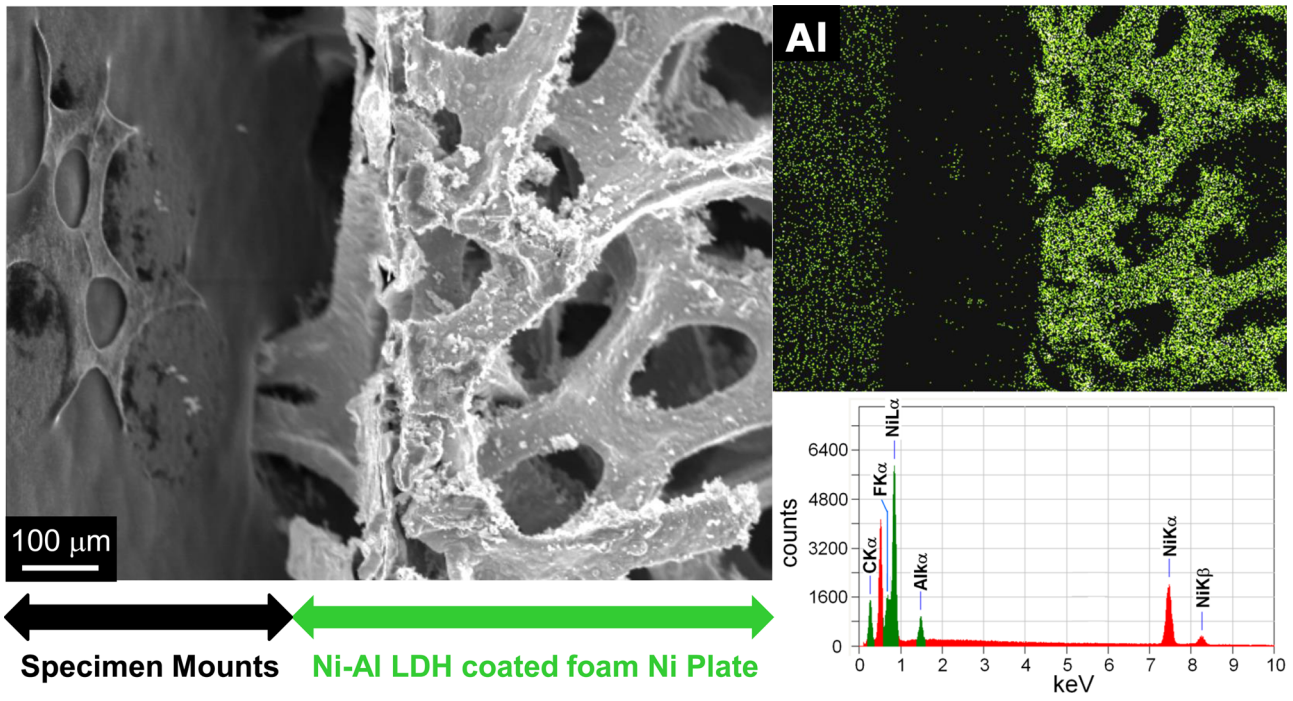

Figure 8. SEM micrograph (left) and corresponding EDX spectrum (top right) for aluminum element of the deposited Ni−Al LDH thin films on the surface of a foam nickel plate. In the EDX spectrum, the amount of aluminum element increases in the order of gray, green, and white dots. The pH of the LPD reaction is 8.5, and the other conditions of the reaction solution are as in Figure 3.

and α-alumina powder. Accordingly, the deposition amount of Ni−Al LDH is also expected to further decrease.

The Ni−Al LDH synthesis by the LPD reaction onto the surface of a foam nickel plate, which was hydrophilized by plasma etching, was carried out. The SEM micrographs and XRD patterns of the pH dependence of the Ni−Al LDH thin films are shown in Figure 7. The high shaping-ability to substrates of the LPD method is high, as the reaction field of the LPD method is a solution system with a short mean free path.[14,39,42−44] Therefore, it can be confirmed from the SEM images that the foam nickel plate surface is completely covered by the extremely minute mesh-like Ni−Al LDH thin film. The sluff of the Ni−Al LDH thin film is minimal, and it is obvious that an excellent deposition was achieved. For the LPD reaction at pH 7.5, a small amount of deposition of the minute mesh-like Ni−Al LDH thin film can be confirmed from the SEM image, whereas no deposition was detected by XRD. It can be estimated that the deposited Ni−Al LDH film thickness is extremely thin. The generation of the secondary particles is hardly observed, which suggests the formation of the Ni−Al LDH thin film on the substrate occurs in the initial stage of the LPD reaction. In the case of the LPD reaction at pH 8.2, the depositions of the Ni−Al LDH thin film on the surface of the foam nickel plate and some secondary particles on the Ni−Al LDH thin film can be observed. The deposition of the Ni−Al LDH thin film was also confirmed by the XRD pattern. The deposition amount of the thin film increases according to an increase in the pH of the LPD reaction solution. As mentioned above, the deposition amount of the Ni−Al LDH on the foam nickel plate surface is considerably less than that on the carbon black powder surface because of the high surface smoothness and the small surface area per unit volume of the foam nickel plate. On the other hand, the widths of detected XRD signals arising from the Ni−Al LDH on the foam nickel plate surface are similar to those on the carbon black powder surface, so the crystallinity of the Ni−Al LDH synthesized by the LPD method is not affected by the material of the substrate. For the LPD reaction at pH 8.5, the further increase of deposition amounts of not only the Ni−Al LDH thin film on the foam nickel plate surface but also Ni−Al LDH secondary particles on the Ni−Al LDH thin film can be confirmed. The active material thin film of a sufficient thickness might provide a three-dimensional electrical conductivity path, whereas the increase of the formation of the secondary particles causes the increase of the charge transfer resistance between active material particles. It can be concluded that the LPD reaction at pH 8.2 is suitable for the preparation of a positive electrode, which exhibits high capacity and low charge transfer resistance. The introduction of trivalent cations, such as Al^{3+} ion, to the LDH mainframe contributes to the stabilization of the α-phase of nickel hydroxide and the improvement of the electrochemical characteristics (e.g., electron and ion conductivities).[4,8,12,13] Therefore, SEM-EDX spectroscopy was employed in this work.

Figure 8 shows the SEM micrograph and the corresponding EDX elemental mapping analysis of the Ni−Al LDH surface that is deposited on the foam nickel plate surface. An adequate amount and uniform distribution of the Al^{3+} ion in the Ni−Al LDH was confirmed; thus, the successful introduction of Al^{3+} ion to the LDH mainframe can be verified. The composition formula of the Ni−Al LDH on the foam nickel plate surface was $Ni_{0.95}Al_{0.05}(OH)_2 \cdot X_{0.05}$ (X means the ion exchangeable OH^- anions between the LDH layers). The Ni^{2+} ion which has been dissolved from the foam nickel plate by hydrofluoric acid is taken into the Ni−Al LDH; hence, it can be estimated that the uptake of aluminum decreases relatively. In addition, the bird's-eye view SEM micrograph of the Ni−Al LDH on the foam nickel plate where the Ni−Al LDH was partially exfoliated from the foam nickel plate is shown in Figure 9. It can be observed that the Ni−Al LDH thin film of about 300 nm of uniform thickness was deposited on the foam nickel plate

DOI: 10.1021/acsami.5b04038
ACS Appl. Mater. Interfaces 2015, 7, 17188−17198

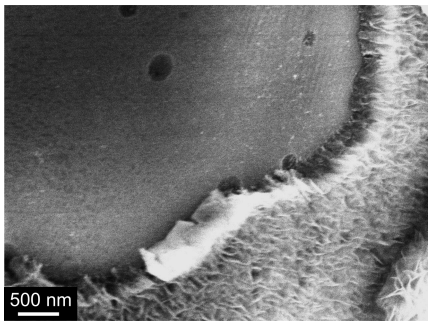

Figure 9. Bird's-eye view SEM micrograph of Ni−Al LDH deposited on a foam nickel plate on which the Ni−Al LDH was partially exfoliated from the foam nickel plate. The pH of the LPD reaction is 8.5, and the other conditions of the reaction solution are as in Figure 3.

surface. There is no gap between the foam nickel plate surface and the deposited Ni−Al LDH thin film, and the construction of the highly adhesive active material thin layer on the surface of substrates is achieved. This deposition of the active material thin layer with high crystallinity and uniform thickness and excellent adhesion onto the electroconductive foam nickel plate surface can be expected to be beneficial for the development toward the interface control of charge transfer reaction fields and the internal resistance reduction of various secondary batteries.[52−55]

The fluoride concentration and the pH dependences of the LPD reaction solution on the surface morphology of the deposited Ni−Al LDH on the foam nickel plate surface, as shown in Figure 10, are important. It should be noted that the

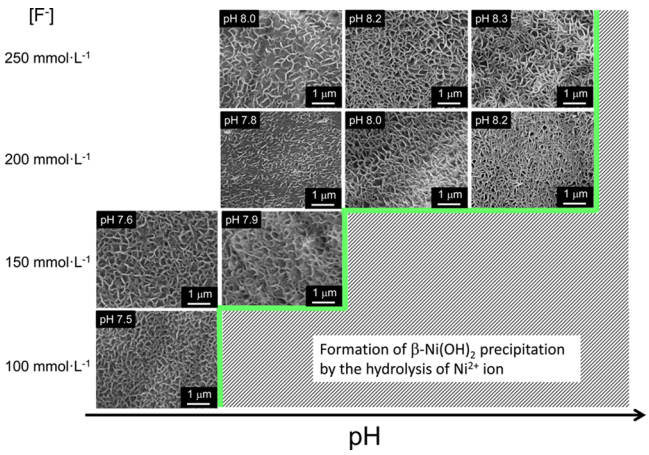

Figure 10. Surface morphologies by SEM of Ni−Al LDH thin films on the surface of foam nickel plates deposited by the LPD reaction at 50 °C for 48 h and obtained at various pH values and total concentrations of fluorine. The concentrations of Ni^{2+} ion and Al^{3+} ion were 12 mmol L^{-1} and 1.2 mmol L^{-1}, respectively.

dependences of the fluoride concentration and the pH of the LPD reaction solution on the surface morphology of the deposited Ni−Al LDH are similar to those on the carbon black powder substrate in spite of the different materials and the shapes of the substrates. Namely, in the SEM images, a minute mesh-like Ni−Al LDH thin film deposited densely on the foam nickel plate surface at the pH range of 7.5 < pH < 8.3, and the surface morphologies and the deposition amounts of the Ni−Al LDH thin films are remarkably influenced by the pH as well as the crystallinity of the Ni−Al LDH.[56] The fineness of the mesh of the deposited Ni−Al LDH thin film is also influenced by the fluoride concentration and the pH of the LPD reaction solution, and the fineness is a minimum at pH 8.2 and $[F^-]$ = 200 mmol L^{-1}. It can be concluded that these conditions of the LPD reaction solution are optimal for the Ni−Al LDH thin film deposition onto the nickel surface. It is noticed that these optimal synthetic conditions for the nickel plate substrate are identical to those determined for the carbon black powder substrate.

In the construction of an optimal electrochemical reaction interface, the membrane thickness control of the active material thin films on current collectors is an indispensable elemental technology. Thus, the Ni−Al LDH thin film deposition on a foam nickel plate surface at various LPD reaction times was carried out in this study. A surface roughness of several micron size on the foam nickel plate surface generated when manufactured by electrodeposition can be observed from the SEM image before the LPD reaction, as shown in Figure S2 (Supporting Information). From the top view SEM micrographs after the LPD reactions after 24 and 48 h, as shown in the upper row of Figure 11 (top), this surface roughness on the

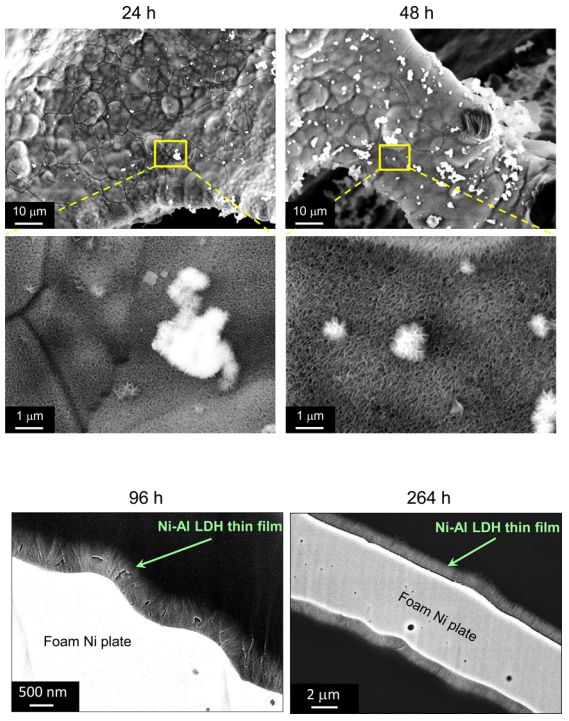

Figure 11. Reaction time dependences of top view SEM micrographs (top) and cross-sectional SEM images (bottom) of the deposited Ni−Al LDH on a foam nickel plate. The pH of the LPD reaction is 8.2, and the concentrations of Ni^{2+} ion and Al^{3+} ion were 12 mmol L^{-1} and 1.2 mmol L^{-1}, respectively, and the total concentrations of fluorine is 200 mmol L^{-1}.

foam nickel plate surface can be seen through the Ni−Al LDH thin film layer. Therefore, this suggests that the deposited Ni−Al LDH thin film thickness is extremely thin when the LPD reaction time is 48 h or less. The deposition of the minute mesh-like Ni−Al LDH thin film of approximately 100 nm over the whole surface of the foam nickel plate can be confirmed from the enlarged top view SEM micrographs, as shown in the lower row of Figure 11 (top). The surface roughness on the foam nickel plate surface can be observed clearly in the case of

DOI: 10.1021/acsami.5b04038
ACS Appl. Mater. Interfaces 2015, 7, 17188−17198

the LPD reaction after 24 h from the enlarged top view SEM micrograph, whereas the surface roughness in the case of the LPD reaction after 48 h is not as clear as that in the case of the LPD reaction after 24 h. This strongly suggests an increase of the Ni−Al LDH thin film thickness with longer reaction time. The deposition of a Ni−Al LDH layer can be observed for the LPD reaction, which exceeds 48 h from the cross-sectional SEM images, as shown in Figure 11 (bottom). There is no gap between the foam nickel plate surface and the deposited Ni−Al LDH thin film, and the highly adhesive active material thin layer to the surface of substrates has been successfully constructed regardless of the LPD reaction time. The reaction field of the LPD method is only the solid−liquid interface. Thus, the LPD reaction always proceeds by the interfacial reaction, and the thin films deposit only on the surface of the solid phase (i.e., the foam nickel plate surface (at the start of the LPD reaction) or the deposited Ni−Al LDH thin film surface (after the start of the LPD reaction)). The deposition of the active material thin film, which has a high crystallinity, a uniform thin film thickness, and an extremely high adhesion to the electric conductive foam nickel plate surface, was achieved. The Ni−Al LDH thin film thickness was determined from the cross-sectional SEM images, and its LPD reaction time dependency is shown in Figure 12. The Ni−Al LDH thin

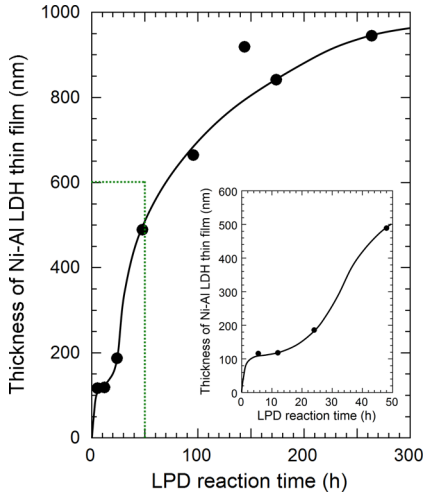

Figure 12. Reaction time dependence of the thickness of the Ni−Al LDH thin films on the surface of foam nickel plates which is determined from each cross-sectional SEM image of the Ni−Al LDHs on a foam nickel plate. The inset figure shows an enlarged view of the area enclosed with the dotted line. The condition of the LPD reaction solution is as shown in Figure 11. Solid lines show smooth curves between data points.

film thickness increases monotonously in accordance with the elapse of the LPD reaction time. However, the rate of increase of the thin film thickness is not constant.[57] The deposition rates of thin films in the LPD reactions usually undergo the following three stages: (1) the deposition rate increases gradually by the progress of the crystal nucleus generation after the start of the LPD reaction; (2) the deposition rate becomes constant by the progress of the crystal nucleus growth; (3) the deposition rate decreases gradually by the decrease of the reaction species concentrations in the LPD reaction solution. It is noteworthy that the rapid Ni−Al LDH thin film deposition on the foam nickel plate surface progresses within 5 h after the start of the LPD reaction, as can be seen from the inset plot in Figure 12. The metal surface, which has a low hydrophilicity, has a significantly different surface free energy as compared with the highly hydrophilic substrate surface (e.g., glass and alumina). The surface free energy changes when the hydrophobic metal surface is covered by the hydrophilic Ni−Al LDH, and the deposition rate of the LDH increases for a while, whereas the surface of the foam nickel plate is always etched by hydrofluoric acid. Therefore, the coating by the Ni−Al LDH on the foam nickel plate surface and the subsequent growth of the LDH thin film will inactivate compared with the case of the alumina and carbon black powder substrates. In addition, because of the high surface smoothness and the small surface area of the foam nickel plate, the deposition rate of the Ni−Al LDH to the foam nickel plate surface is considerably slower than that to the hydrophilized carbon black powder surface. The above-described three stages of the Ni−Al LDH thin film deposition progress. Namely, the LDH thin film thickness increases rapidly over about 20 h after the start of the LPD reaction and becomes constant at 950 nm after about 250 h, because neither the nickel nor aluminum were supplied during the LPD reaction in this research. As a result, the active material layer thickness was able to be controlled within the range from 100 nm to 1 μm by the LPD reaction time, so it can be expected that it is possible to apply this technique to the optimization of the interface structure of the charge transfer reaction field between a current collector and an active material.

4. CONCLUSIONS

The hydrolysis reaction and the fluoride ion consumption reaction in the LPD reaction, which had been empirically carried out, were clarified by the theoretical approach from the viewpoint of the complexation and solution equilibria of the dissolved species in the LPD reaction. The yields of metal oxides and hydroxides by the LPD method were very sensitive to the supersaturation state of the hydroxide in the reaction solution, and this theoretical approach can be used as a benchmark of the optimal conditions of the fluoride concentration and the pH for the LPD reaction of the Ni−Al LDH synthesis. The optimal conditions of the LPD reaction solution (i.e., pH 8.2 and $[F^-]$ = 200 mmol L^{-1}) enabled the high yield synthesis of the high crystallinity and density Ni−Al LDH regardless of the material of substrates, because the LPD method is a reaction in solution using the minute free energy difference between two complexation equilibria as a driving force for the progress of the reaction. Therefore, the information about the optimal conditions for the LPD reaction solution can be widely applied to not only various metal oxide and hydroxide thin film depositions but also the versatile control of various reaction interfaces on substrates. There is no gap between the surfaces of conductive substrates (i.e., carbon black powder and foam nickel plate) and the deposited Ni−Al LDH thin film. Hence, the highly adhesive active material thin layer to various electroconductive substrates was successfully constructed. Furthermore, the active material layer thickness could be controlled within the range from 100 nm to 1 μm by the LPD reaction time. The depositions of the high-crystallinity and the arbitrary-thickness active material thin films, which have excellent adhesion onto the foam nickel plate surface as a current collector, can be expected to be beneficial for the development of the interface control of charge transfer reaction fields and the internal resistance reduction of various secondary batteries.

DOI: 10.1021/acsami.5b04038
ACS Appl. Mater. Interfaces 2015, 7, 17188−17198

■ ASSOCIATED CONTENT

Supporting Information

Figure S1: Stability constants of various metal-fluoro complexes concerning the LPD reactions, Figure S2: SEM micrograph of a foam nickel plate (Sumitomo Electric Industries, Ltd., Celmet #8) before the LPD reaction. Mean bore diameter is 0.45 mm, specific surface area is 291 cm^2 g^{-1}, and porosity is 98%, Scheme S1: Preparation of Ni parent solution for the synthesis of Ni−Al LDH by the LPD process. The Supporting Information is available free of charge on the ACS Publications website at DOI: 10.1021/acsami.5b04038.

■ AUTHOR INFORMATION

Corresponding Author

*E-mail: maki@kobe-u.ac.jp.

Notes

The authors declare no competing financial interest.

■ ACKNOWLEDGMENTS

This study was carried out under the Technology Development of Energy Storage System for Grid Stabilization Projects; "Development of Safety and Cost Competitive Energy Storage System for Renewable Energy" supported by Kawasaki Heavy Industries, Ltd. and New Energy and Industrial Technology Development Organization (NEDO) and the Japan Society for the Promotion of Science (JSPS) KAKENHI Grant-in-Aid for Scientific Research (C) (No.15K05644).

■ REFERENCES

(1) Morishita, M.; Shimizu, Y.; Kobayakawa, K.; Sato, Y. Suppression of the Memory Effect Observed in Alkaline Secondary Batteries under Partial Charge−Discharge Conditions. *Electrochim. Acta* **2008**, *53*, 6651−6656.

(2) Delahaye-Vidal, A.; Figlarz, M. Textural and Structural Studies on Nickel Hydroxide Electrodes. II. Turbostratic Nickel (II) Hydroxide Submitted to Electrochemical Redox Cycling. *J. Appl. Electrochem.* **1987**, *17*, 589−599.

(3) Sugimoto, A.; Ishida, S.; Hanawa, K. Preparation and Characterization of Ni/Al-Layered Double Hydroxide. *J. Electrochem. Soc.* **1999**, *146*, 1251−1255.

(4) Gao, Z.; Wang, J.; Li, Z.; Yang, W.; Wang, B.; Hou, M.; He, Y.; Liu, Q.; Mann, T.; Yang, P.; Zhang, M.; Liu, L. Graphene Nanosheet/Ni^{2+}/Al^{3+} Layered Double-Hydroxide Composite as a Novel Electrode for a Supercapacitor. *Chem. Mater.* **2011**, *23*, 3509−3516.

(5) Wang, Y.; Zhang, D.; Peng, W.; Liu, L.; Li, M. Electrocatalytic Oxidation of Methanol at Ni−Al Layered Double Hydroxide Film Modified Electrode in Alkaline Medium. *Electrochim. Acta* **2011**, *56*, 5754−5758.

(6) Kamath, P. V.; Dixit, M.; Indira, L.; Shukla, A. K.; Kumar, Y. G.; Munichandraiah, N. Stabilized α-$Ni(OH)_2$ as Electrode Material for Alkaline Secondary Cells. *J. Electrochem. Soc.* **1994**, *141*, 2956−2959.

(7) Liu, Q.; Fan, G.; Zhang, S.; Liu, Y.; Li, F. Synthesis of Uniform Ni−Al Layered Double Hydroxide via a Novel Reduction−Oxidation Route. *Mater. Lett.* **2012**, *82*, 4−6.

(8) Béléké, A. B.; Mizuhata, M. Electrochemical Properties of Nickel−Aluminum Layered Double Hydroxide/Carbon Composite Fabricated by Liquid Phase Deposition. *J. Power Sources* **2010**, *195*, 7669−7676.

(9) Béléké, A. B.; Higuchi, E.; Inoue, H.; Mizuhata, M. Durability of Nickel−Metal Hydride (Ni−MH) Battery Cathode Using Nickel−Aluminum Layered Double Hydroxide/Carbon (Ni−Al LDH/C) Composite. *J. Power Sources* **2014**, *247*, 572−578.

(10) Mizuhata, M.; Hosokawa, A.; Béléké, A. B.; Deki, S. Ni−Al Layered Double Hydroxide Prepared by Liquid Phase Deposition. *Chem. Lett.* **2009**, *38*, 972−973.

(11) Béléké, A. B.; Hosokawa, A.; Mizuhata, M.; Deki, S. Preparation of α-nickel Hydroxide/Carbon Composite by the Liquid Phase Deposition Method. *J. Ceram. Soc. Jpn.* **2009**, *117*, 392−394.

(12) Béléké, A. B.; Higuchi, E.; Inoue, H.; Mizuhata, M. Effects of the Composition on the Properties of Nickel-Aluminum Layered Double Hydroxide/Carbon (Ni-Al LDH/C) Composite Fabricated by Liquid Phase Deposition(LPD). *J. Power Sources* **2013**, *225*, 215−220.

(13) Morishita, M.; Kakeya, T.; Ochiai, S.; Ozaki, T.; Kawabe, Y.; Watabe, M.; Sakai, T. Structural Analysis by Synchrotron X-ray Diffraction, X-ray Absorption Fine Structure and Transmission Electron Microscopy for Aluminum-Substituted α-type Nickel Hydroxide Electrode. *J. Power Sources* **2009**, *193*, 871−877.

(14) Maki, H.; Mori, Y.; Okumura, Y.; Mizuhata, M. Anion-Exchange Properties of Nickel-Aluminum Layered Double Hydroxide Prepared by Liquid Phase Deposition. *Mater. Chem. Phys.* **2013**, *141*, 445−453.

(15) Allmann, R. Doppelschichtstrukturen mit Brucitähnlichen Schichtionen $[Me(II)_{1-x}Me(III)_x(OH)_2]^{x+}$. *Chimia* **1970**, *24*, 99−108.

(16) Duan, X.; Evans, D. G. *Layered Double Hydroxide*, 1st ed.; Springer: Berlin, 2006; Chapter 2, pp 119.

(17) Jitianu, M.; Gunness, D. C.; Aboagye, D. E.; Zaharescu, M.; Jitianu, A. Nanosized Ni−Al Layered Double Hydroxides-Structural Characterization. *Mater. Res. Bull.* **2013**, *48*, 1864−1873.

(18) Ahmed, A. A. A.; Talib, Z. A.; Hussein, M. Z.; Zakaria, A. Zn−Al Layered Double Hydroxide Prepared at Different Molar Ratios: Preparation, Characterization, Optical and Dielectric Properties. *J. Solid State Chem.* **2012**, *191*, 271−278.

(19) Oliver-Tolentino, M.; Vázquez-Samperio, J.; Manzo-Robledo, A.; González-Huerta, R. G.; Flores-Moreno, J. L.; Ramírez-Rosales, D.; Guzmán-Vargas, A. An Approach to Understanding the Electrocatalytic Activity Enhancement by Superexchange Interaction toward OER in Alkaline Media of Ni−Fe LDH. *J. Phys. Chem. C* **2014**, *118*, 22432−22438.

(20) Carvalho, H. W. P.; Pulcinelli, S. H.; Santilli, C. V.; Leroux, F.; Meneau, F.; Briois, V. XAS/WAXS Time-Resolved Phase Speciation of Chlorine LDH Thermal Transformation: Emerging Roles of Isovalent Metal Substitution. *Chem. Mater.* **2013**, *25*, 2855−2867.

(21) Aisawa, S.; Kudo, H.; Hoshi, T.; Takahashi, S.; Hirahara, H.; Umetsu, Y.; Narita, E. Intercalation Behavior of Amino Acids into Zn−Al-Layered Double Hydroxide by Calcination−Rehydration Reaction. *J. Solid State Chem.* **2004**, *177*, 3987−3994.

(22) Feng, Z.; Yang, Z.; Yang, B.; Zhang, Z.; Xie, X. The Application of Co−Al-Hydrotalcite as a Novel Additive of Positive Material for Nickel−Metal Hydride Secondary Cells. *J. Power Sources* **2014**, *266*, 22−28.

(23) Aisawa, S.; Takahashi, S.; Ogasawara, W.; Umetsu, Y.; Narita, E. Direct Intercalation of Amino Acids into Layered Double Hydroxides by Coprecipitation. *J. Solid State Chem.* **2001**, *162*, 52−62.

(24) Leroux, F.; Besse, P. J. Polymer Interleaved Layered Double Hydroxide: A New Emerging Class of Nanocomposites. *Chem. Mater.* **2001**, *13*, 3507−3515.

(25) Kubo, D.; Tadanaga, K.; Hayashi, A.; Tatsumisago, M. Hydroxide Ion Conduction in Ni−Al Layered Double Hydroxide. *J. Electroanal. Chem.* **2012**, *671*, 102−105.

(26) Aisawa, S.; Hirahara, H.; Uchiyama, H.; Takahashi, S.; Narita, E. Synthesis and Thermal Decomposition of Mn−Al Layered Double Hydroxides. *J. Solid State Chem.* **2002**, *167*, 152−159.

(27) Yamaguchi, N.; Nakamura, T.; Tadanaga, K.; Matsuda, A.; Minami, T.; Tatsumisago, M. Platelike Crystal Growth of Zn−Al Layered Double Hydroxide by Hot Water Treatment of Sol−Gel Derived Al_2O_3−ZnO Films on Glass Substrate. *Chem. Lett.* **2006**, *35*, 174−175.

(28) Chubar, N.; Gerda, V.; Megantari, O.; Mičušík, M.; Omastova, M.; Heister, K.; Man, P.; Fraissard, J. Applications versus Properties of Mg−Al Layered Double Hydroxides Provided by Their Syntheses Methods: Alkoxide and Alkoxide-Free Sol−Gel Syntheses and Hydrothermal Precipitation. *Chem. Eng. J.* **2013**, *234*, 284−299.

(29) Zhang, F.; Du, N.; Song, S.; Liu, J.; Hou, W. Mechano-Hydrothermal Synthesis of Mg_2Al−NO_3 Layered Double Hydroxides. *J. Solid State Chem.* **2013**, *206*, 45−50.

DOI: 10.1021/acsami.5b04038
ACS Appl. Mater. Interfaces 2015, 7, 17188−17198

(30) Chen, S.-K.; Chiu, K.-F.; Su, S.-H.; Liu, S.-H.; Hou, K. H.; Leu, H.-J.; Hsiao, C.-C. Low Contact Resistance Carbon Thin Film Modified Current Collectors for Lithium Ion Batteries. *Thin Solid Films* **2014**, *572*, 56−60.
(31) Wu, H.-C.; Wu, H.-C.; Lee, E.; Wu, N.-L. High-Temperature Carbon-Coated Aluminum Current Collector for Enhanced Power Performance of $LiFePO_4$ Electrode of Li-Ion Batteries. *Electrochem. Commun.* **2010**, *12*, 488−491.
(32) Jeong, B.; Uhm, S.; Kim, J.-H.; Lee, J. Pyrolytic Carbon Infiltrated Nanoporous Alumina Reducing Contact Resistance of Aluminum/Carbon Interface. *Electrochim. Acta* **2013**, *89*, 173−179.
(33) Taer, E.; Deraman, M.; Talib, I. A.; Hashmi, S. A.; Umar, A. A. Growth of Platinum Nanoparticles on Stainless Steel 316L Current Collectors to Improve Carbon-Based Supercapacitor Performance. *Electrochim. Acta* **2011**, *56*, 10217−10222.
(34) Lei, C.; Markoulidis, F.; Ashitaka, Z.; Lekakou, C. Reduction of Porous Carbon/Al Contact Resistance for an Electric Double-Layer Capacitor (EDLC). *Electrochim. Acta* **2013**, *92*, 183−187.
(35) Deki, S.; Yoshida, N.; Hiroe, Y.; Akamatsu, K.; Mizuhata, M.; Kajinami, A. Growth of Metal Oxide Thin Films from Aqueous Solution by Liquid Phase Deposition Method. *Solid State Ionics* **2002**, *151*, 1−9.
(36) Maki, H.; Okumura, Y.; Ikuta, H.; Mizuhata, M. Ionic Equilibria for Synthesis of TiO_2 Thin Films by the Liquid-Phase Deposition. *J. Phys. Chem. C* **2014**, *118*, 11964−11974.
(37) Deki, S.; Aoi, Y.; Hiroi, O.; Kajinami, A. Titanium (IV) Oxide Thin Films Prepared from Aqueous Solution. *Chem. Lett.* **1996**, *25*, 433−434.
(38) Deki, S.; Aoi, Y.; Okibe, J.; Yanagimoto, H.; Kajinami, A.; Mizuhata, M. Preparation and Characterization of Iron Oxyhydroxide and Iron Oxide Thin Films by Liquid-Phase Deposition. *J. Mater. Chem.* **1997**, *7*, 1769−1772.
(39) Deki, S.; Nakata, A.; Miyake, T.; Ooka, S.; Mizuhata, M. Nanofabrication Process for Highly Ordered Porous Materials by the Liquid Phase Deposition Methods. *ECS Trans.* **2007**, *6*, 11−22.
(40) Wang, B.; Williams, G. R.; Chang, Z.; Jiang, M.; Liu, J.; Lei, X.; Sun, X. Hierarchical NiAl Layered Double Hydroxide/Multiwalled Carbon Nanotube/Nickel Foam Electrodes with Excellent Pseudocapacitive Properties. *ACS Appl. Mater. Interfaces* **2014**, *6*, 16304−16311.
(41) Fujita, R.; Sakairi, M.; Kikuchi, T.; Nagata, S. Corrosion Resistant TiO_2 Film Formed on Magnesium by Liquid Phase Deposition Treatment. *Electrochim. Acta* **2011**, *56*, 7180−7188.
(42) Aoi, Y.; Kambayashi, H.; Deguchi, T.; Yato, K.; Deki, S. Synthesis of Nanostructured Metal Oxide by Liquid-Phase Deposition. *Electrochim. Acta* **2007**, *53*, 175−178.
(43) Deki, S.; Iizuka, S.; Horie, A.; Mizuhata, M.; Kajinami, A. Liquid-Phase Infiltration (LPI) Process for the Fabrication of Highly Nano-Ordered Materials. *Chem. Mater.* **2004**, *16*, 1747−1750.
(44) Deki, S.; Iizuka, S.; Horie, A.; Mizuhata, M.; Kajinami, A. Nanofabrication of Metal Oxide Thin Films and Nano-Ceramics from Aqueous Solution. *J. Mater. Chem.* **2004**, *14*, 3127−3132.
(45) Smith, R. M.; Martell, A. E. *Critical Stability Constants, Vol. 4: Inorganic Complexes*; Prenum Press: New York, 1976; p 96.
(46) Högfeldt, E. *Stability Constants of Metal-ion Complexes Part A: Inorganic Ligands*; Pergamon Press: Oxford, 1982.
(47) Kuratani, K.; Mizuhata, M.; Kajinami, A.; Deki, S. Synthesis and Luminescence Property of Eu^{3+}/ZrO_2 Thin Film by the Liquid Phase Deposition Method. *J. Alloys Compd.* **2006**, *408−412*, 711−716.
(48) Ciavatta, L.; Pirozzi, A. The Formation of Flouride Complexes of Titanium(IV). *Polyhedron* **1983**, *2*, 769−774.
(49) Pearson, R. G. Hard and Soft Acids and Bases. *J. Am. Chem. Soc.* **1963**, *85*, 3533−3539.
(50) Edwards, J. O. Correlation of Relative Rates and Equilibria with a Double Basicity Scale. *J. Am. Chem. Soc.* **1954**, *76*, 1540−1547.
(51) Jensen, W. B. The Lewis Acid-Base Definitions: a Status Report. *Chem. Rev.* **1978**, *78*, 1−22.
(52) Miyazaki, K.; Asada, Y.; Fukutsuka, T.; Abe, T.; Bendersky, L. A. Structural Insights into Ion Conduction of Layered Double Hydroxides with Various Proportions of Trivalent Cations. *J. Mater. Chem. A* **2013**, *1*, 14569−14576.
(53) Wang, B.; Liu, Q.; Qian, Z.; Zhang, X.; Wang, J.; Li, Z.; Yan, H.; Gao, Z.; Zhao, F.; Liu, L. Two Steps in situ Structure Fabrication of Ni−Al Layered Double Hydroxide on Ni Foam and Its Electrochemical Performance for Supercapacitors. *J. Power Sources* **2014**, *246*, 747−753.
(54) Ji, K.; Xu, C.; Zhao, H.; Dai, Z. Electrodeposited Lead-Foam Grids on Copper-Foam Substrates as Positive Current Collectors for Lead-Acid Batteries. *J. Power Sources* **2014**, *248*, 307−316.
(55) Wu, H.-C.; Lin, Y.-P.; Lee, E.; Lin, W.-T.; Hu, J.-K.; Chen, H.-C.; Wu, N.-L. High-Performance Carbon-Based Supercapacitors Using Al Current-Collector with Conformal Carbon Coating. *Mater. Chem. Phys.* **2009**, *117*, 294−300.
(56) Song, Q.; Tang, Z.; Guo, H.; Chan, S. L. I. Structural Characteristics of Nickel Hydroxide Synthesized by a Chemical Precipitation Route under Different pH Values. *J. Power Sources* **2002**, *112*, 428−434.
(57) Deki, S. Fabrication of Advanced Materials from Aqueous Solution. *GS News Technol. Rep.* **2003**, *62*, 46−53.

DOI: 10.1021/acsami.5b04038
ACS Appl. Mater. Interfaces 2015, 7, 17188−17198